Euromech 262 – Sand Transport in Rivers, Estuaries and the Sea, Soulsby & Bettess (eds)
 ISBN 90 6191 186 9

Sediment transport in combined currents and waves

L.C.van Rijn
Delft Hydraulics, Netherlands

ABSTRACT: Sediment concentration profiles in waves and currents measured in flume and field conditions are analyzed. A new engineering method to compute time-averaged concentration profiles and the depth-integrated transport rate is given. Comparison of measured and computed transport rates shows reasonably good agreement.

1. INTRODUCTION

Wave motion over a movable fine sand bed (50 to 500 μm) can generate a sediment suspension with relatively large sediment concentrations in the near-bed region as shown by Nakato et al (1977) and by Bosman (1982) for the ripple regime and by Horikawa et al (1982) and by Staub et al (1984) for the plane bed (sheet flow) regime. When tide-induced, wind-induced or wave-induced currents are present, additional mixing over the water depth will be generated resulting in an increase of the sediment concentrations in the upper layers. The basic mechanism of sediment suspension and transport in combined current and waves is the entrainment of particles by the stirring action of the waves and the transport of the particles by the current motion. The transport of particles by the mean current velocities (in the presence of waves) is herein defined as the current-related transport rate.

In this paper concentration profiles measured in flume and field conditions are analyzed and discussed.

A new engineering method to compute time-averaged concentration profiles and depth-integrated transport rates in combined currents and waves is presented.

The total sediment transport rate (q_t) can be computed from the vertical distribution of fluid velocities and sediment concentrations, as follows:

$$q_t = \int_0^{h+\eta} UC \, dz \tag{1}$$

in which:
- U = local instantaneous fluid velocity at height z above bed
- C = local instantaneous sediment concentration at height z above bed
- h = water depth (to mean surface level)
- η = water surface elevation

Defining: $U = u + \tilde{u}$ and $C = c + \tilde{c}$ (2)

in which:
- u = time and space-averaged fluid velocity at height z
- c = time and space-averaged concentration at height z
- $\tilde{u}$ = oscillating fluid component (including turbulent component)
- $\tilde{c}$ = oscillating concentration component (including turbulent component)

Substituting Eq. (2) in Eq. (1) and averaging over time and space, yields:

$$\bar{q}_t = \int_0^h uc \, dz + \int_0^h \overline{\tilde{u}\tilde{c}} \, dz = \bar{q}_c + \bar{q}_w \tag{3}$$

in which:

$\bar{q}_c = \int_0^h uc \, dz$ = time-averaged current-related sediment transport rate

$\bar{q}_w = \int_0^h \overline{\tilde{u}\tilde{c}} \, dz$ = time-averaged wave-related sediment transport rate

The current-related sediment transport is defined as the transport of sediment particles by the time-averaged (mean) current velocities (longshore currents, rip currents, undertow currents). The current velocities and the sediment concentrations are affected by the wave motion. It is known that the wave motion reduces the current velocities near the bed, but the wave motion strongly increases the near-bed concentrations due to its stirring action. The wave-related sediment transport is defined as the transport of sediment particles by the oscillating fluid components (cross-shore orbital motion).

The oscillating components ($\tilde{u}$ and $\tilde{c}$) may also be affected by the current velocities.

2. TRANSPORT PROCESSES IN WAVES

2.1 Instantaneous concentrations

Instantaneous concentrations are especially important with respect to the wave-related transport processes. Instantaneous concentrations generated by non-breaking waves in the <u>ripple</u> regime have been measured by Nakato et al (1977) and by Bosman (1982).
Instantaneous concentrations in the plane bed (sheet flow) regime have been measured by Horikawa et al (1982) and by Staub et al (1984).

Figure 1 shows ensemble mean concentrations within a wave period in a wave tunnel measured by Bosman (1982) for an experiment in the ripple regime. A sinusoidal oscillatory motion with a period of T = 1 sec and a velocity amplitude of $\hat{U}_\delta$ = 0.3 m/s was generated over sand bed (d_{50} = 200 µm, d_{90} = 240 µm). The bed was covered with almost perfectly two-dimensional ripples (length = 0.055 m, height = 0.01 m). An optical instrument was used to measure the concentrations above the ripple crest and the trough. The exact measuring locations are shown in Fig. 1. The ripple crest measurements show ensemble mean concentrations and standard deviations based on 100 periods. About 70% of all measurements are within the standard deviation lines. As regards the trough measurements, only ensemble mean values are shown. The following phenomena can be observed above the crest:

- the (random) scatter is quite large (roughly ± 50%),
- two large concentration peaks just after flow reversal and probably generated by leeside eddy-velocities,
- two smaller concentration peaks at the moment of maximum flow, probably generated by stoss-side velocities,
- asymmetrical concentration distribution (water motion is symmetrical).

The phenomena above the trough are:

- the (random) scatter is also quite large (not shown),
- two larger concentration peaks after flow reversal and probably generated by leeside eddy-velocities (time lag is larger compared with concentration measurements at the crest)
- two smaller concentration peaks after maximum flow and probably generated by stoss-side velocities,
- asymmetrical concentration distribution,
- the peaks above the trough are smaller than those above the crest due to dispersion and settling of sediment particles.

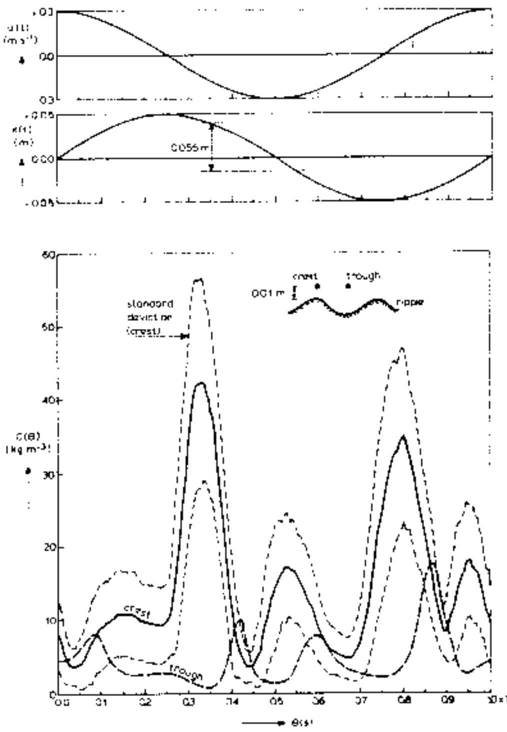

Fig. 1 Instantaneous concentrations in ripple regime

According to Bosman (1982), the scatter is mainly caused by (slight) local ripple changes resulting in small differences in the local velocities and hence concentrations. Based on this, it seems very difficult to relate the local instantaneous sediment concentration to a local instantaneous fluid velocity. The measurements of Nakato et al (1977) with periods in the range of 1 to 3 s show similar results as those of Bosman.
Mathematical models to compute the instantaneous sediment concentrations in the ripple regime are not yet available.

Instantaneous concentrations generated by non-breaking waves in the <u>sheet flow regime</u> have been measured by Horikawa et al (1982) in oscillatory flow over a sand bed (d_{50} = 200 µm) in a wave tunnel using an electro-resistance concentration meter. Large concentrations gradients were observed in a layer of 0.003 to 0.005 m above and below the initial bed surface level. The maximum concentrations were generated at the moment of maximum velocities. The concentrations were minimum at the moment of minimum velocities. The thickness of the concentration layer was about 0.02 m. At this latter level the time-averaged concentration was about 0.5 kg/m³. Analysis of the instantaneous sand transport

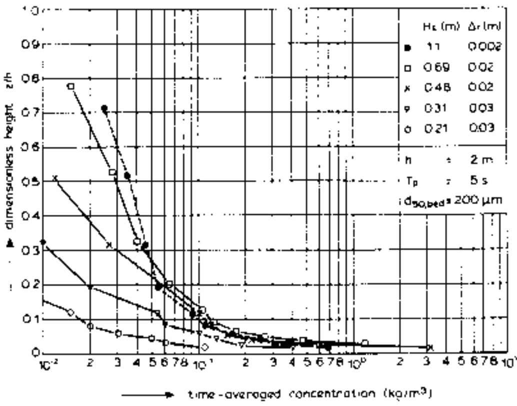

Fig. 2 Time-averaged concentrations in non-breaking waves

rates shows that most of the transport occurs below the initial bed level.

2.2 Time-averaged concentrations

Time-averaging is necessary to eliminate the large random scatter of the instantaneous concentrations in the ripple regime. Time-averaged concentrations have been measured by various researchers.
Figure 2 shows time-averaged concentrations measured by Van Rijn (1987) using a pump sampler in a large-scale wave flume with a water depth of 2 m and a sand bed with d_{50} = 210 µm. Irregular (non-breaking) waves were generated. The bed was covered with pronounced ripples with a height of about 0.02 m for H_s = 0.69 m, (H_s = significant wave height); smooth ripples with a height of 0.001 m were observed after the test with $H_s \geq 1.1$ m.

The following phenomena were observed:

- increasing concentrations for increasing wave height upto H_s = 0.69 m and decreasing concentrations for H_s = 1.1 m in the near-bed layer,
- two layer concentration profiles with large gradients in the near-bed layer of $z/h < 0.05$ (3 ripple heights) and small gradients for $z/h > 0.05$,
- decrease of ripple height from Δ_r = 0.02 m to 0.001 m for wave height increasing from H_s = 0.69 m to H_s = 1.1 m

The experimental results indicate a simultaneous decrease of the near-bed concentrations and the ripple height when the wave height increases from H_s = 0.69 m to H_s = 1.1 m. This can be observed more clearly in Fig. 3 showing the concentrations at three elevations (z = 0.025 h, 0.05 h and 0.1 h) as a function of the

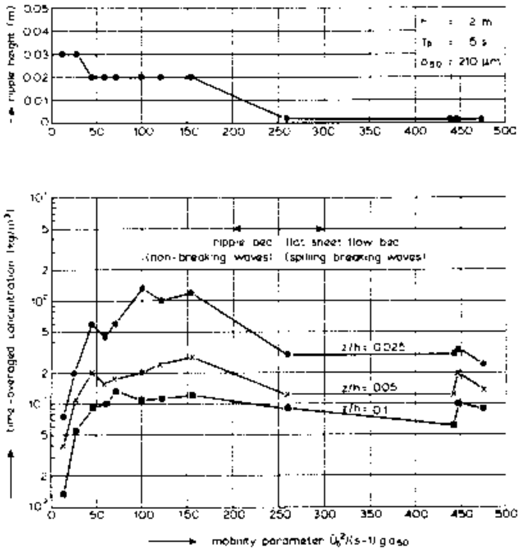

Fig. 3 Bedform height and concentrations in non-breaking waves

mobility parameter $\psi = \hat{U}_\delta^2/[(s-1)gd_{50}]$ in which $\hat{U}_\delta$ = amplitude of near-bed orbital velocity and $s = \rho_s/\rho$. The ripple height is also plotted as a function of ψ. Figure 3 clearly shows that the concentrations are largest for ψ = 150 in the presence of ripples with a height of 0.02 m. For ψ > 150 there is a gradual transition from the ripple regime (height = 0.02 m) with relative large concentrations to the smooth bed regime (smooth flat ripples of 0.001 m) with relatively small concentrations. It is most likely that the ripple-generated eddies, which are most effective in the entrainment of particles from the bed, are gradually disappearing for ψ = 150 resulting in gradual decrease of the concentrations, as shown in Fig. 3.

The effect of breaking waves can be clearly observed in Fig. 4 presenting the experimental results of Bosman (1982), measured in a wave flume at a water depth of 0.3 m and a sand bed of d_{50} = 100 µm. Irregular waves were generated. According to Bosman (1982), the bed was flat at locations near the breaking waves.

Two phenomena can be observed:

- the near-bed concentrations are approximately constant ($\simeq$ 10 kg/m³) for increasing wave heights,
- the concentrations at higher levels show a large increase for wave heights increasing from H_s = 0.12 m (non-breaking waves) to H_s = 0.19 m (plunging breaking waves).

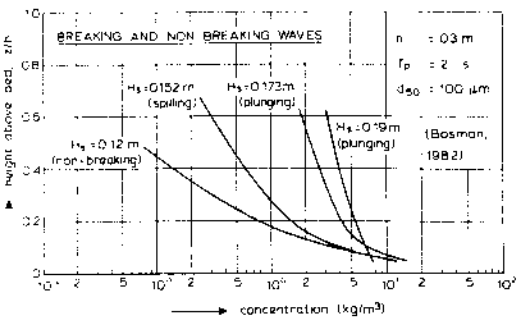

Fig. 4 Concentration profiles in breaking waves

Observations have shown that bed forms are washed out when the mobility parameter ψ is larger than about 200 to 250. In that case a thin (- 0.03 m) layer of moving sediment particles with high concentrations close to the bed is generated. This is called the sheet flow layer. Time-averaged concentrations in the sheet flow layer have only been measured in wave tunnel experiments (Horikawa et al, 1982; Staub et al, 1984 and Ribberink, 1989). Field data are not available.

2.3 Computation of time-averaged concentration profiles

2.3.1 Basic equation

Usually, the convection-diffusion equation is applied to compute the equilibrium concentration profile in steady flow. This equation reads as:

$$w_{s,m} c + \varepsilon_s \frac{dc}{dz} = 0 \qquad (4)$$

in which:

$w_{s,m}$ = particle fall velocity of suspended sediment in a fluid-sediment mixture,

ε_s = sediment mixing coefficient,

c^5 = time-averaged concentration at height z above the bed.

Here, it is assumed that Eq. (4) is also valid for wave-related mixing.

2.3.2 Sediment mixing coefficient for non-breaking waves

Measurements in wave flumes show the presence of suspended sediment particles from the bed upto the water surface (Bosman, 1982; Van Rijn, 1987). The largest concentrations are found close to the bed where the diffusivity is large due to ripple-generated eddies. Further away from the bed the sediment concentrations decrease

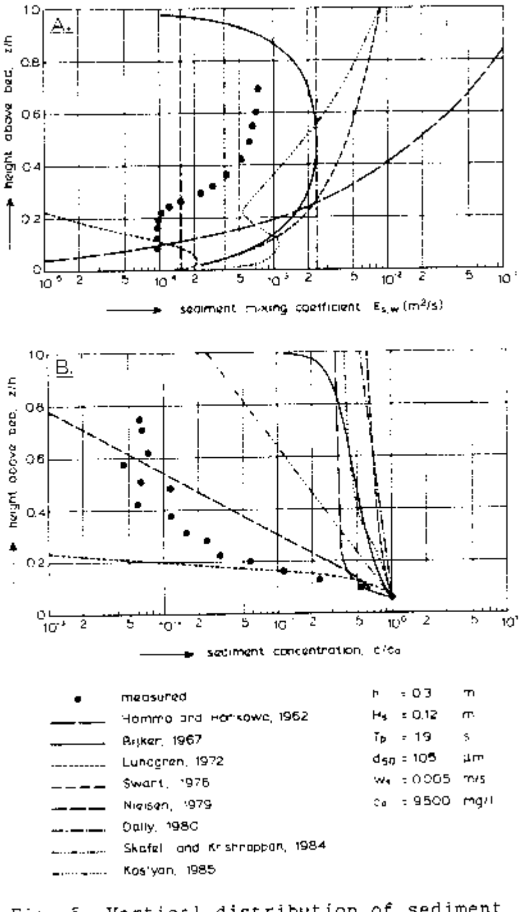

Fig. 5 Vertical distribution of sediment mixing coefficient and concentration

rapidly because the eddies dissolve rather rapidly travelling upwards.

Various researchers have tried to model the suspension process by introducing an effective wave-related sediment mixing coefficient: Homma - Horikawa (1962), Bijker (1967, 1971), Lundgren (1972), Bhattacharya (1971), Swart (1976), Nielsen (1979), Dally (1980), Skafel-Krishnappan (1984) and Kos'yan (1985).

The proposed relationships were used by the author to compute the wave-related sediment mixing coefficient distribution for an experiment of Bosman (1982).

The results are shown in Figure 5A. The "measured" values represent the sediment mixing coefficients derived from the measured sediment concentration profile, which is shown in Figure 5B. The "measured" values indicate a constant sediment mixing coefficient in the near-bed region. Above this region the sediment mixing coefficient increases rather strongly upto the mid-depth level. In the upper half of the water depth the measured sediment mixing coefficient is approximately constant. None of the proposed relationships has a distribution similar to that of the measured values. Most expressions yield values which are much too large. The expression proposed by Nielsen produces a mixing coefficient of the right order of magnitude in the near-bed region. The expression of Lundgren, which only represents the turbulence-related mixing process in the boundary layer, also yields values of the right order of magnitude in the near-bed region. Outside the boundary layer (δ_w = 0.015 m) the sediment mixing coefficient of Lundgren decreases rapidly. Figure 5B shows measured and computed concentration profiles for the same experiment. The computed concentrations are based on a numerical solution of the diffusion equation applying the proposed expressions for the sediment mixing coefficient. The concentration measured in the lowest sampling point was used as bed boundary concentration (c_a = 9500 mg/l at z = 0.02 m) for the numerical computation of the concentration profile. The concentration profile based on the sediment mixing coefficient of Lundgren shows reasonable results in the near-bed region ($z < 0.2$ h). Outside the boundary layer the concentrations decrease much too rapidly. Comparing the results of the other methods, the Nielsen method yields the most reasonable results. The methods of Homma-Horikawa, Bijker, Swart, Dally, Skafel-Krishnappan and Kos'yan produce incorrect results.

As the existing relationships do not yield acceptable results, a new approach is presented here. Based on analysis of measured concentration profiles the following characteristics were observed (Van Rijn, 1989):

- approximately constant mixing coefficient ($\varepsilon_{s,w,bed}$) in a layer ($z \leq \delta_s$) near the bed,
- approximately constant mixing coefficient ($\varepsilon_{s,w,max}$) in the upper half ($z \geq 0.5$ h) of the water depth,
- approximately linear variation for $\delta_s < z < 0.5$ h.

The mathematical formulation reads as:

$$z \leq \delta_s \qquad \varepsilon_{s,w} = \varepsilon_{s,w,bed} \tag{5a}$$

$$z \geq 0.5\,h \qquad \varepsilon_{s,w} = \varepsilon_{s,w,max} \tag{5b}$$

$$\delta_s < z < 0.5\,h \qquad \varepsilon_{s,w} = \varepsilon_{s,w,bed} + [\varepsilon_{s,w,max} - \varepsilon_{s,w,bed}]\left[\frac{z-\delta_s}{0.5h-\delta_s}\right] \tag{5c}$$

Equation (5) is fully defined when the following three parameters are known:

1. thickness of near-bed sediment mixing layer (δ_s),
2. mixing coefficient near the bed ($\varepsilon_{s,w,bed}$),
3. mixing coefficient in the upper half of the depth ($\varepsilon_{s,w,max}$).

1. Thickness of near-bed sediment mixing layer (δ_s)

Analysis of concentration profiles measured by Bosman (1982) shows the presence of a near-bed layer with an almost constant mixing coefficient (Fig. 5B). The thickness of this layer is about 0.03 to 0.05 m, which is approximately 3 to 6 times the ripple height.

In case of a flat bed (sheet flow) the effective sediment mixing layer δ_s will be proportional to the wave boundary layer δ_w. Here, it is assumed that:

$$\delta_s = 3\,\Delta_r \quad \text{(ripple regime)}$$

$$\delta_s = 3\,\delta_w \quad \text{(sheet flow regime)} \tag{6}$$

in which:

Δ_r = ripple height,
δ_w = $0.072\,\hat{A}_\delta\,(\hat{A}_\delta/k_{s,w})^{-0.25}$ = wave boundary layer thickness,
δ_s = thickness of near-bed sediment mixing layer,
$k_{s,w}$ = wave-related bed roughness height (= $3\Delta_r$ in ripple regime and 30 d_{90} in sheet flow regime).

2. Mixing coefficient in near-bed layer ($\varepsilon_{s,w,bed}$)

Basically, the mixing coefficient is defined as the product of a length scale and a velocity scale, as follows:

$$\varepsilon_{s,w} = L\,U \tag{7}$$

In case of oscillatory flow near the bed it seems logic to assume:

$$\varepsilon_{s,w,bed} = \alpha_b\,\hat{U}_\delta\,\delta_s \tag{8}$$

in which:

α_b = empirical coefficient,
$\hat{U}_\delta$ = peak value of near-bed orbital velocity,
δ_s = thickness of near-bed sediment mixing layer.

Sediment concentration measurements in waves alone of Nieuwjaar (1987), Van Rijn (1987), Bosman (1982) and Van der Velden (1986) were used to determine the α_b-coefficient, yielding:

$$\alpha_b = 0.004\,D_*$$

with:

$D_* = d_{50}[[(\rho_s - \rho)g]/(\rho\nu^2)]^{1/3}$ = particle size parameter.

3. Mixing coefficient in upper layer ($\varepsilon_{s,w,max}$)

For the upper layer it is assumed that:

$$\varepsilon_{s,w,max} \approx \hat{W}_{0.5h}\, h \tag{9}$$

in which:
$\hat{W}_{0.5h}$ = peak value of vertical orbital velocity at mid-depth level,
h = water depth.

From linear wave theory it follows that:

$$W_{0.5h} \approx \frac{H}{T} \tag{10}$$

Combining Equations (9) and (10) it follows that:

$$\varepsilon_{s,w,max} = \alpha_m \frac{h\,H}{T} \quad \text{for } z/h \geq 0.5 \tag{11}$$

in which:
α_m = empirical coefficient found to be 0.035.

Analysis of measured concentration profiles has shown that the vertical distribution of the mixing coefficients for breaking waves is quite similar to that for non-breaking waves (Van Rijn, 1989). Based on this similarity of the vertical distribution of the mixing coefficients, a simple approach is proposed by introducing a breaking coefficient (α_{br}) which acts as a multiplier on the mixing coefficient for non-breaking waves, as follows:

$$\varepsilon_{s,w,br} = \alpha_{br}\, \varepsilon_{s,w} \tag{12}$$

in which:
$\varepsilon_{s,w,br}$ = sediment mixing coefficient in case of breaking waves,
$\varepsilon_{s,w}$ = sediment mixing coefficient in case of non-breaking waves,
α_{br} = breaking coefficient.

The α_{br}-coefficient is assumed to be constant over the depth and to be dependent on the breaker type.
As a first approach, the following relationship is proposed:

$$\alpha_{br} = 3\left[\frac{H_s}{h}\right] - 0.8 \quad \text{for} \quad \frac{H_s}{h} > 0.6 \tag{13}$$

2.3.3 Reference concentration in near-bed region

For unidirectional steady flow the author (Van Rijn, 1984) has proposed a simple deterministic expression to compute the reference concentration, which reads as:

$$c_a = 0.015\, \frac{d_{50}}{a}\, \frac{T^{1.5}}{D_*^{0.3}} \tag{14}$$

in which:
D_* = dimensionless particle diameter (-),
T = $[\bar{\tau}'_{b,c} - \bar{\tau}_{b,cr}]/\bar{\tau}_{b,cr}$ = dimensionless bed-shear parameter (-),
$\bar{\tau}'_{b,c}$ = $\mu_c\, \bar{\tau}_{b,c}$ = current-related effective bed-shear stress (N/m²),
$\bar{\tau}_{b,cr}$ = critical bed-shear stress according to Shields (N/m²),
c_a = reference concentration (-).

Equation (14) is assumed to be valid for oscillatory flow as well, applying an effective wave-related bed shear stress, as follows:

$$\bar{\tau}'_{b,w} = \mu_w\, \bar{\tau}_{b,w} \tag{15}$$

in which:
$\bar{\tau}'_{b,w}$ = wave-related effective bed-shear stress (N/m²),
μ_w = wave-related efficiency factor (-),
$\bar{\tau}_{b,w}$ = wave-related bed-shear stress (N/m²).

The wave-related bed-shear stress is computed as:

$$\bar{\tau}_{b,w} = \frac{1}{4}\,\rho\, f_w\, (\hat{U}_\delta)^2 \tag{16}$$

in which:
f_w = $\exp[-6 + 5.2\,(\hat{A}_\delta/k_{s,w})^{-0.19}]$,
$f_{w,max}$ = 0.3,
$k_{s,w}$ = wave-related bed-roughness (= 3 Δ_r in ripple regime and 30 d_{90} in sheet flow regime),
Δ_r = ripple height
$\hat{U}_\delta$ = peak value of near-bed orbital velocity,
$\hat{A}_\delta$ = peak value of near-bed orbital excursion.

The efficiency factor (μ_w) was determined by calibration using measured concentrations giving:

$$\mu_w = \frac{0.6}{D_*} \tag{17}$$

Now, the reference level is discussed. In case of a bed form regime it is proposed to apply the reference level at the crest level of the bed forms, which means that the reference level (a) is equal to half the bed form height. Thus a = 0.5 Δ_r.
In case of sheet flow conditions with a flat bed it is proposed to apply the reference level at the outer edge of the sheet flow layer, which means that the reference level is equal to the thickness of the wave boundary layer. Thus a = δ_w.

The sediment particles below the reference level are assumed to be transported as bed load.

2.3.4 Concentration profile

Applying Eqs. (4) and (5) and neglecting the hindered settling effect, the vertical distribution of the concentration can be obtained by integration, yielding:

$\underline{a \le z < \delta_s}$

$$\frac{c}{c_a} = [e]^{w_s(a-z)/\varepsilon_{s,w,bed}} \tag{18a}$$

$\underline{\delta_s \le z < 0.5h}$

$$\frac{c}{c_a} = [e]^{w_s(a-\delta_s)/\varepsilon_{s,w,bed}} \times$$

$$\times \left[\frac{h}{h + \gamma(z - \delta_s)}\right]^{w_s h/(\gamma\, \varepsilon_{s,w,bed})} \tag{18b}$$

$\underline{0.5h \le z \le h}$

$$\frac{c}{c_a} = [e]^{w_s(a-\delta_s)/\varepsilon_{s,w,bed}} \times$$

$$\times \left[\frac{h}{h+\gamma(0.5h-\delta_s)}\right]^{w_s h/(\gamma\, \varepsilon_{s,w,bed})} \times$$

$$\times [e]^{w_s(0.5h-z)/\varepsilon_{s,w,max}} \tag{18c}$$

in which:

γ $= \left[\frac{h}{0.5h - \delta_s}\right]\left[\frac{\varepsilon_{s,w,max} - \varepsilon_{s,w,bed}}{\varepsilon_{s,w,bed}}\right]$

= coefficient

c_a = reference concentration according to Eq. (14)

a = reference level

h = water depth to still water level

δ_s = thickness of near-bed mixing layer according to Eq. (6)

$\varepsilon_{s,w,bed}$ = sediment mixing coefficient in near-bed region, Eq. (8)

$\varepsilon_{s,w,max}$ = sediment mixing coefficient in upper layer, Eq. (11)

w_s = particle fall velocity in clear water

z = vertical coordinate above bed.

The characteristics wave parameters are assumed to be the significant wave height (H_s) and the peak period (T_p).

Figure 6 shows computed and measured concentration profiles for large-scale flume experiments (Van Rijn, 1989). Water depths were in the range of 2 to 3 m. The bed material size was about 220 µm. The bed was almost flat in case of large waves ($H_s/h > 0.4$), while ripples with a height of about $\Delta_r = 0.02$ m were present in case of small waves ($H_s/h < 0.4$). The wave-related bed roughness height in all experiments was estimated as: $k_{s,w} = 3\ d_{90} + 3\ \Delta_r$.

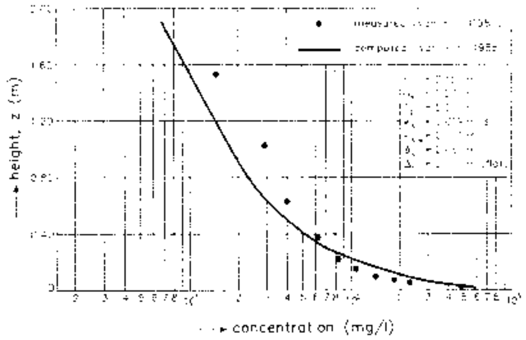

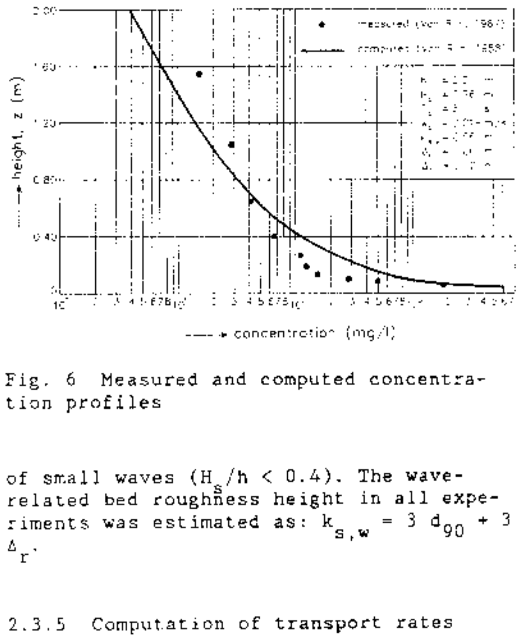

Fig. 6 Measured and computed concentration profiles

2.3.5 Computation of transport rates

Since the major part of the sediment suspension in wave conditions is confined to a region close to the bed (within 3 to 5 times the ripple height or the sheet flow layer thickness), it seems logic to compute the wave-related sediment transport by a simple formula in analogy with the bed load transport formulae applied in steady currents. A division between bed load and suspended load only is of academic interest.
The author proposes to determine the time-averaged transport rate (in m²/s) over half the wave period in non-breaking waves as $\bar{q}_w = \alpha_1 a c_a \hat{U}_\delta$ with α_1 = calibration coefficient.
Applying Eq. (14) the following expression can be derived:

$$\bar{q}_w = \alpha_1\ a\ c_a\ \hat{U}_\delta = \alpha_2\ d_{50}\ \hat{U}_\delta\ T^{1.5}\ D_*^{-0.3} \tag{19}$$

in which:

T = dimensionless bed-shear stress parameter, see Eq. (14)
D_* = dimensionless particle parameter,
$\hat{U}_\delta$ = peak value of near-bed orbital velocity,
d_{50} = median particle diameter of bed material,
a = δ_w = reference level (= wave boundary layer thickness),
α_2 = calibration coefficient (= 0.03).

The calibration coefficient was determined from the sheet flow measurements of Ribberink and Al Salem (1991), giving $\alpha_2 = 0.03$ (using $k_{s,w} = 0.01$ m).

The net time-averaged wave-induced transport rate in asymmetrical oscillatory motion is given by:

$$\bar{q}_{w,net} = \bar{q}_{w,max} - \bar{q}_{w,min} = \alpha_2\, d_{50}\, D_*^{-0.3} \left[\hat{U}_{\delta,max}\, T_{max}^{1.5} - \hat{U}_{\delta,min}\, T_{min}^{1.5}\right] \qquad (20)$$

Equation (20) is only valid for non-breaking wave conditions. The maximum and minimum peak orbital velocities can be obtained from second order Stokes theory. In case of breaking wave conditions there is a net offshore-directed current in the lower part of the water depth (undertow). The current-related transport by the undertow should be added to the wave-related transport according to Eq. (20).

3. TRANSPORT PROCESSES IN COMBINED CURRENTS AND WAVES

3.1 Time-averaged concentration profiles

Figure 7 shows examples of time-averaged concentrations measured by Nieuwjaar-Van der Kaaij, 1987 for a similar water depth of 0.5 m and 100 μm-sediment. Irregular waves were generated. In all tests the bed was covered with ripples.

The following phenomena were observed:

- rapid decrease of concentrations in lower layers in case of waves alone ($\bar{u} = 0$ m/s),
- transport of sediment to upper layers by mixing effects in case of combined waves and currents,
- mixing effects are small in case of a weak current ($\bar{u} = 0.1$ m/s), and large in case of a strong current ($\bar{u} = 0.4$ m/s),
- influence of current direction (following or opposing) on concentration profile is relatively small,
- influence of current velocity on the near-bed concentrations, which are in the range of 0.1 to 10 kg/m³, is only significant in case of small waves.

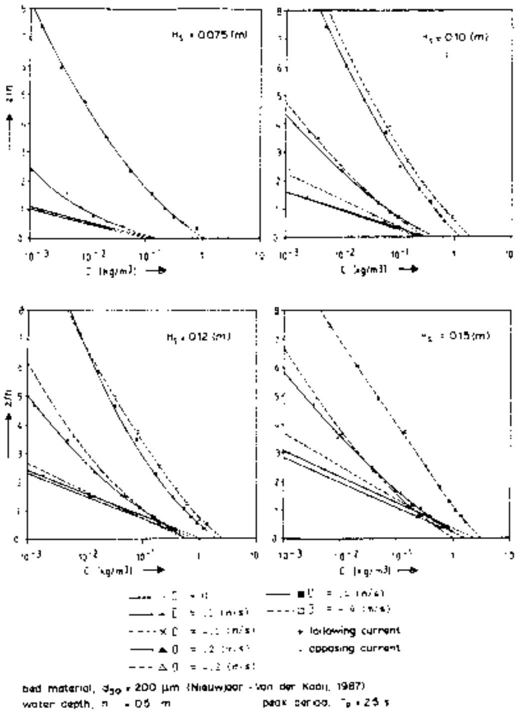

Fig. 7 Concentration profiles in combined currents and waves

Time-averaged concentrations in the surf zone (USA) with breaking waves have been measured by Jaffe et al (1984) using an optical sampler and by Van Rijn (1987) using a pump sampler.

The following phenomena were observed in the surf zone:

- near-bed concentrations in the range of 0.1 to 2 kg/m³ for relative wave heights in the range of H_s/h = 0.3 to 0.7,
- relatively large vertical mixing due to wave-related and current-related mixing in the longshore trough area and at the longshore bar area,
- presence of smooth bottom undulations with a height in the order of 0.01 to 0.02 m in cross-shore direction in case of spilling breaking waves (H_s/h = 0.3 to 0.4).

The main cause for the relatively small near-bed concentrations (0.1 to 2 kg/m³) in the surf zone is the absence of the typical wave-induced bed ripples and the associated eddies. Wave-induced eddies near ripples are strong stirring mechanisms yielding large near-bed concentrations (1 to 10 kg/m³) at relatively small wave heights, as shown by laboratory experiments.

3.2 Computation of time-averaged concentration profiles

3.2.1 Basic equations

Various models to compute time-averaged concentration profiles are available in the literature. The Bijker model (1967, 1971) is based on the time-averaged convection-diffusion equation (Eq. 4). Other models such as that of Fredsøe et al (1985) and that of Deigaard et al (1986) are based on the instantaneous convection-diffusion equation. These latter models are only valid for plane bed conditions with sheet flow.

Since reliable models to predict the time-averaged concentration profiles for a rippled bed or a plane sheet flow bed are still lacking, the present author proposes hereafter a new engineering method based on the time-averaged mixing coefficients. The method is valid for non-breaking and breaking waves over a rippled or a plane bed.

The concentration profile can be obtained from numerical integration of the time-averaged convection-diffusion Equation (4) applying Equation (14) as reference concentration:

$$\frac{dc}{dz} = \frac{c\ w_{s,m}}{\varepsilon_{s,cw}} \tag{21}$$

in which:

c = time-averaged concentration at height z above the bed (-)
$w_{s,m}$ = $(1-c^5)\ w_s$ = particle fall velocity of suspended sediment in fluid-sediment mixture (m/s)
w_s = particle fall velocity of suspended sediment in clear water (m/s)
$\varepsilon_{s,cw}$ = sediment mixing coefficient in combined currents and waves (m²/s)

3.2.2 Sediment mixing coefficient

The sediment mixing coefficient in combined currents and waves is assumed to be given by:

$$\varepsilon_{s,cw} = [\varepsilon_{s,c}^2 + \varepsilon_{s,w}^2]^{0.5} \tag{22}$$

in which:

$\varepsilon_{s,w}$ = wave-related mixing coefficient according to Eqs. (5), (8), (11).
$\varepsilon_{s,c}$ = current-related mixing coefficient.

The current-related mixing coefficient reads as:

$$\varepsilon_{s,c} = \kappa\ \beta\ u_{*,c}\ z(1-z/h) \quad \text{for} \quad z < 0.5\ h \tag{23a}$$

$$\varepsilon_{s,c} = 0.25\ \beta\ \kappa\ u_{*,c}\ h \quad \text{for} \quad z \geq 0.5\ h \tag{23b}$$

in which:

$u_{*,c}$ = $(g^{0.5}\ \bar{v}_R)/C$ = bed-shear velocity
C = $18\log(12h/k_{s,c})$ = Chézy-coefficient
$\bar{v}_R$ = depth-averaged velocity
$k_{s,c}$ = current-related bed-roughness height
h = water depth
κ = constant of Von Karman (= 0.4)
β = coefficient ($\simeq$ 1).

3.2.3 Reference concentration

The reference concentration is given by:

$$c_a = 0.015\ \frac{d_{50}}{a}\ \frac{T^{1.5}}{D_*^{0.3}} \tag{24}$$

in which:

D_* = dimensionless particle parameter (-),
T = dimensionless bed-shear stress parameter (-),
a = reference level (m).

The T-paramter is as follows:

$$T = (\bar{\tau}'_{b,cw} - \bar{\tau}_{b,cr})/\bar{\tau}_{b,cr} \tag{25}$$

in which:

$\bar{\tau}'_{b,cw}$ = time-averaged effective bed-shear stress (N/m²)
$\bar{\tau}_{b,cr}$ = time-averaged critical bed-shear stress according to Shields (N/m²)

The magnitude of the time-averaged bed-shear stress, which is independent of the angle between the wave- and current direction (Van Rijn, 1990), is given by:

$$\bar{\tau}'_{b,cw} = \bar{\tau}'_{b,c} + \bar{\tau}'_{b,w} \tag{26}$$

in which:

$\bar{\tau}'_{b,c}$ = $\mu_c\ \alpha_{cw}\ \bar{\tau}_{b,c}$ = current-related effective bed-shear stress (N/m²)
$\bar{\tau}'_{b,w}$ = wave-related effective bed-shear stress according to Eq. (16) (N/m²)
$\bar{\tau}_{b,c}$ = $\rho g(\bar{v}_R/C_{ap})^2$ = current-related bed shear stress
μ_c = $(C/C')^2$ = efficiency factor
C_{ap} = $18\log(12h/k_a)$
C' = $18\log(12h/3\ d_{90})$, $C = 18\log(12h/k_{s,c})$
$\bar{v}_R$ = depth-averaged velocity
k_a = apparent current-related bed roughness height, see Eq. (29)
$k_{s,c}$ = physical current-related bed roughness height
α_{cw} = $\left[\frac{\ln(90\ \delta_w/k_a)}{\ln(90\ \delta_w/k_{s,c})}\right]^2$ = wave-current interaction coefficient representing reduced velocity-effect near the bed, see Eq. (29).

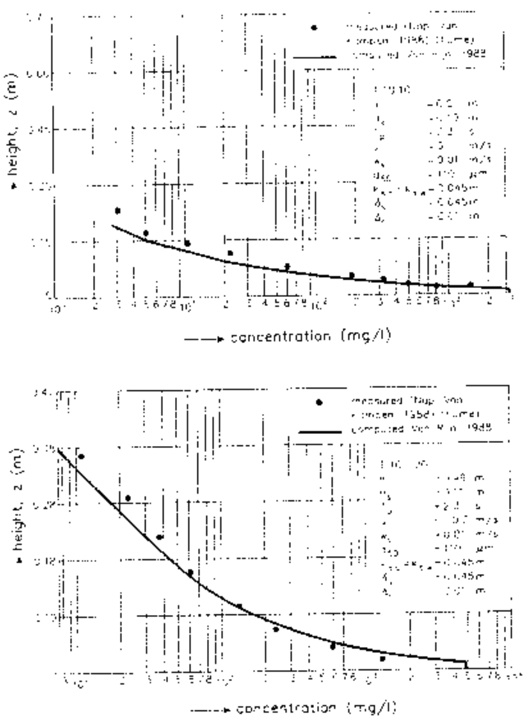

Fig. 8 Measured and computed concentrations in a flume

$$\delta_w = 0.072\ \hat{A}_\delta (\hat{A}_\delta / k_{s,w})^{-0.25}$$ = thickness of wave boundary layer

The reference level is assumed to be equal to $a = 0.5\ \Delta_r$ in case of a rippled bed (Δ_r = ripple height) or $a = \delta_w$ in case of a plane sheet flow bed (δ_w = wave boundary layer thickness).

3.2.4 Examples

Figure 8 shows examples of measured and computed concentration profiles for non-breaking irregular waves in a flume (sand bed, d_{50} = 200 µm). Figure 9 shows measured and computed concentration in the surf zone with longshore velocities upto 0.5 m/s (Jaffe et al, 1984).

3.3 Computation of transport rates

The current-related bed-load transport ($\bar{q}_{b,c}$) and the current-related suspended-load transport ($\bar{q}_{s,c}$) as modified by the wave motion are herein presented. The total transport is defined as the sum of the current-related and the wave-related transport.

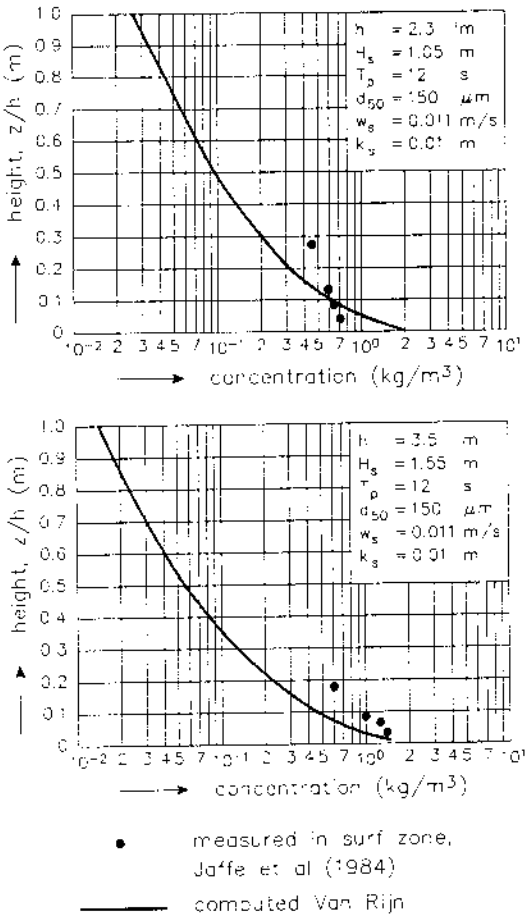

Fig. 9 Measured and computed concentrations in surf zone

3.3.1 Current-related bed-load transport:

The bed-load transport is given by (Van Rijn, 1989):

$$\bar{q}_{b,c} = 0.25\ u'_{*,c}\ d_{50}\ T^{1.5}\ D_*^{-0.3} \tag{27}$$

in which:

$\bar{q}_{b,c}$ = time-averaged bed-load transport (m^2/s)
$u'_{*,c} = (g^{0.5} \bar{v}_R)/C'$ = current-related grain bed-shear velocity (m/s)
d_{50} = median particle diameter of bed material (m)
T = dimensionless bed-shear stress parameter due to current and waves (-)
D_* = dimensionless particle parameter (-)

$C' = 18 \log(12h/3d_{90})$ = grain-related Chézy-coefficient ($m^{0.5}/s$)

The T-parameter is a stirring parameter governing the entrainment of the bed material particles whereas the $u'_{*,c}$-parameter acts as a transport parameter. Equation (27) which is valid for particles in the range of 100 to 500 μm, yields zero-transport rate when the current velocity is zero.

3.3.2 Current-related suspended load transport

The suspended-load transport is computed by numerical integration over the depth of the product of velocity and concentration, as follows (Van Rijn, 1989):

$$\bar{q}_{s,c} = \int_a^h v_R c \, dz \tag{28}$$

in which:

$\bar{q}_{s,c}$ = time-averaged suspended load transport (m^2/s)
v_R = resultant current velocity at height z above the bed (in the direction of the velocity vector) (m/s)
c = sediment concentration at height z above bed (-)
a = reference level (m)
h = water depth (m)

The concentration profile follows from Eqs. (21), (22) and (24).

The velocity profile is described by:

$$v_{R,z} = \frac{\bar{v}_R \ln(30z/k_a)}{-1 + \ln(30h/k_a)} \quad \text{for } z \geq 3\,\delta_w \tag{29a}$$

$$v_{R,z} = \frac{\bar{v}_R \ln(90\delta_w/k_a)\ln(30z/k_{s,c})}{[-1 + \ln(30h/k_a)][\ln(90\delta_w/k_{s,c})]} \quad \text{for } z < 3\,\delta_w \tag{29b}$$

$k_a = k_{s,c} \exp[\gamma\, \hat{U}_\delta/\bar{v}_R]$ = apparent bed roughness

$k_{a,max} = 10\, k_{s,c}$

with:
$\gamma = 0.75$ for $\phi = 0°$
$\gamma = 0.75$ for $\phi = 90°$
$\gamma = 1.1$ for $\phi = 180°$
(linear interpolation for intermediate values).

Equation (29) represents the velocity profile for a current in the presence of waves. Laboratory observations have shown that the near-bed current velocities are reduced by the wave motion (Van Rijn,

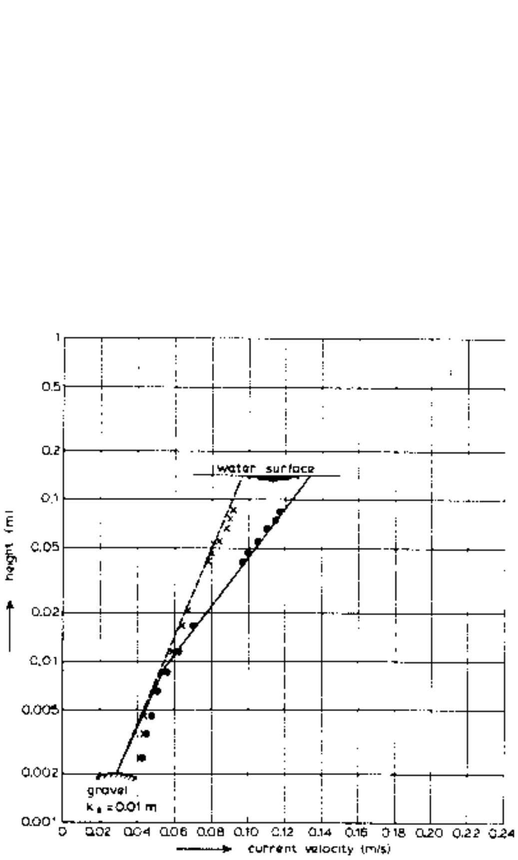

Fig. 10 Measured and computed velocities (x current alone, o current and waves, ϕ = 90°)

1989). This effect can be represented by introducing an apparent bed roughness k_a which affects the outer layer ($z \geq 3\delta_w$). Inside the mixing layer ($z < 3\delta_w$) the velocities are affected by the physical bed roughness $k_{s,c}$ (Van Rijn, 1989). Figure 10 shows an example for combined currents and waves (ϕ = 90°) in a wave basin.

An approximate solution of Eq. (28) is given by:

$$\bar{q}_{s,c} = (F_c + F_w)\, \bar{v}_R\, h\, c_a \tag{30}$$

in which:

current-related correction factor:

$$F_c = \frac{[a/h]^{ZC} - [a/h]^{1.2}}{[1.2-ZC]\,[1-(a/h)]^{ZC}}$$

wave-related correction factor:

$$F_w = \frac{[a/h]^{ZW} - [a/h]^{1.2}}{[1.2-ZW]\,[1-(a/h)]^{ZW}}$$

current-related suspension number:

$$ZC = \frac{w_s}{\beta\, \kappa\, u_{*,c}}$$

wave-related suspension number:

$$ZW = \alpha \left[\frac{w_s}{\bar{v}_R}\right]^{0.9} \left[\frac{\bar{v}_R\, T_p'}{H_s}\right]^{1.05}$$

$\alpha = 7$ for $h \geq 100\ \delta_s$

$\alpha = 0.7(h/\delta_s)^{0.5}$ for $h < 100\ \delta_s$

H_s = significant wave height
T_p' = peak period of wave spectrum (relative to current)
h = water depth
δ_s = thickness of mixing layer near bed (= 0.01 to 0.1 m)

The ZW-number is based on computer fitting using the results of 500 computations with $150 < d_{50} < 400$ µm, $1 < h < 20$ m, $0.1 < \bar{v}_R < 1.5$ m/s, $0.1 < H_s/h < 0.5$ and $a = 0.01\ h$.

Figure 11 shows measured and computed suspended load transport rates according to the method of Van Rijn. The measured values were derived from velocity and concentration measurements in a flume with 100 µm and 200 µm sediment (Nieuwjaar-Van der Kaaij, 1987 and Nap-Van Kampen, 1988). Based on analysis of measured velocity profiles, the effective bed roughness was found to be in the range of 3 to 6 time the ripple height. The computed results of Fig. 11 are based on a value of 3 times the ripple height ($k_{s,c} = k_{s,w} = 3\ \Delta_r$).

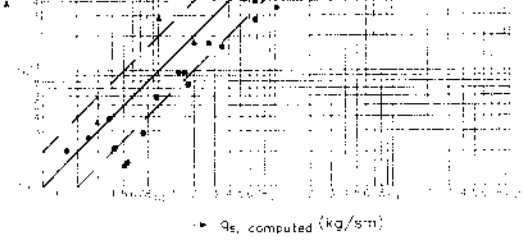

Fig. 11

As can be observed, the measured and computed transport rates show reasonable good agreement. Most (80%) of the computed values are within a factor 2 of the measured values. On the average the computed values are somewhat too large.

3.3.3 Total sediment transport

The total time-averaged sediment transport rate ($\bar{q}_t$) in a current super-imposed by waves can be obtained by vector addition, as follows:

$$\bar{q}_t = [(\bar{q}_c)^2 + (\bar{q}_w)^2 + 2\ |\bar{q}_c|\bar{q}_w|\cos\phi]^{0.5} \tag{31}$$

in which:

$\bar{q}_c$ = $\bar{q}_{b,c} + \bar{q}_{s,c}$ = total current-related transport rate
$\bar{q}_{b,c}$ = current-related bed-load transport rate
$\bar{q}_{s,c}$ = current-related suspended load transport rate
$\bar{q}_w$ = $\int_0^h \overline{\tilde{u}\ \tilde{c}}\ dz = \bar{q}_{w,max} - \bar{q}_{min}$
= net wave-related sediment transport rate in the direction of the largest bed-shear stress.
$\bar{q}_{w,max}$ = $\alpha\ \hat{U}_{\delta,max}\ \delta_{w,max}\ c_{a,max}$
= $\alpha_2\ d_{50}\ D_*^{-0.3}\ \hat{U}_{\delta,max}\ T_{max}^{1.5}$
$\bar{q}_{w,min}$ = $\alpha\ \hat{U}_{\delta,min}\ \delta_{w,min}\ c_{a,min}$
= $\alpha_2\ d_{50}\ D_*^{-0.3}\ \hat{U}_{\delta,min}\ T_{min}^{1.5}$
α = coefficient (= 0.03)
ϕ = angle between wave and current direction
T_{max} = $(\bar{\tau}'_{b,cw,max} - \bar{\tau}_{b,cr})/\ \bar{\tau}_{b,cr}$
T_{min} = $(\bar{\tau}'_{b,cw,min} - \bar{\tau}_{b,cr})/\ \bar{\tau}_{b,cr}$
$\bar{\tau}'_{b,cw,max}$ = $[(\bar{\tau}'_c)^2 + (\bar{\tau}'_{w,max})^2 + 2|\bar{\tau}'_c|\ |\bar{\tau}'_{w,max}|\cos\phi]^{0.5}$
$\bar{\tau}'_{b,cw,min}$ = $[(\bar{\tau}'_c)^2 + (\bar{\tau}'_{w,min})^2 - 2|\bar{\tau}'_c|\ |\bar{\tau}'_{w,min}|\cos\phi]^{0.5}$
$\bar{\tau}'_{w,max}$ = $\frac{1}{4}\ \rho\ \mu_w\ f_{w,max}\ (\hat{U}_{\delta,max})^2$
$\bar{\tau}'_{w,min}$ = $\frac{1}{4}\ \rho\ \mu_w\ f_{w,min}\ (\hat{U}_{\delta,min})^2$

$\hat{U}_{\delta,max}$ and $\hat{U}_{\delta,min}$ are the maximum peak orbital velocity (in wave propagation direction) and the minimum peak orbital velocity (against wave propagation direction) according to higher order Stokes theory (to account for wave asymmetry).

This method yields a net wave-related transport rate in case of combined current and waves, even if the waves are sinusoidal ($\hat{U}_{\delta,max} = \hat{U}_{\delta,min} = \hat{U}_{\delta}$) because there is interaction of the current and waves.

4. REFERENCES

Bhattacharya, P.K. 1971, Sediment Suspension in Shoaling Waves, Ph.D. Thesis, University of Iowa, Iowa City, USA.

Bosman, J., 1982, The Influence of Bottom Slope, Water Depth, Breaking Waves, Orbital Velocity and Current Velocity on the Concentration Distribution under Waves and Currents (in Dutch), Delft Hydraulics, Report M1875, Delft, The Netherlands.

Bijker, E.W., 1967, Some Considerations about Scales for Coastal Models with Movable Bed, Dissertation, Delft Univ. of Technology, Delft, The Netherlands.

Bijker, E.W., 1971, Longshore Transport Computations. Journal of Waterways, Harbour and Coastal Eng., Vol. 99.

Deigaard, R., Fredsøe, J. and Hedegaard, I.B., 1986, Suspended Sediment in Surf Zone, Journal of Waterway, Port, Coastal and Ocean Engineering, Vol. 112, No. 1.

Fredsøe, J., Andersen, O.H. and Silberg, S., 1985, Distribution of Suspended Sediment in Large Waves, Journal of Waterway, Port, Coastal and Ocean Engineering, Vol. 111, No. 6.

Homma, M. and Horikawa, K., 1962, Suspended Sediment due to Wave Action, Proc. 8th Coastal Eng. Conf. Mexico.

Horikawa, K., Watanabe, A. and Katori, S., 1982, Sediment Transport Under Sheet Flow Condition, Coastal Engineering Conference, Houston, USA.

Jaffe, B.E., Sternberg, R.W. and Sallenger, A.H., 1984, The Role of Suspended Sediment in Shore-Normal Beach Profile Changes, Coastal Engineering Conference, Houston, USA.

Kennedy, J.F. and Locher, F.A., 1972, Sediment Suspension by Waves, In: Waves on Beaches by R.E. Meyer, Academic Press.

Kos'yan, R.D., 1985, Vertical Distribution of Suspension Sediment Concentrations Seawards of the Breaking Zone, Coastal Engineering, 9 p. 171-187.

Lundgren, H., 1972, Turbulent Currents in the Presence of Waves, Coastal Eng. Conf., Vancouver, Canada, pp. 623-634.

Nakato, T., Locher, F.A., Glover, J.R. and Kennedy, J.F., 1977, Wave Entrainment of Sediment From Ripples, Journal of Waterways, Port, Coastal and Ocean Div., ASCE, No. WW1.

Nap, E. and Van Kampen, A., 1988, Sediment Transport in Irregular Non-Breaking Waves, Coastal Eng. Dep., Delft Univ. of Technology, Delft, The Netherlands.

Nielsen, P., 1979, Some Basic Concepts of Wave Sediment Transport, Series Papers 20, Inst. of Hydrodyn. and Hydr. Eng., Techn. Univ. of Denmark, Lyngby, Denmark.

Nielsen, P., 1984, On the Motion of Suspended Sand Particles, Journal of Geophysical Research, Vol. 89, No. C1.

Nieuwjaar, M. and Van der Kaaij, Th., 1987, Sediment Concentrations and Transport in Irregular Non-Breaking Waves, Coastal Eng. Dep., Delft Univ. of Technology, Delft, The Netherlands.

Ribberink, J.S., 1989, Sediment Concentration and Bed Regime Measurements in Large Wave Tunnel, Report H840.22, Delft Hydraulics, Delft, The Netherlands.

Ribberink, J.S. and Al Salem, A., 1991, Sediment Transport, Concentrations and Bed Forms in Simulated Asymmetric Wave Conditions, Report H 840-IV, Delft Hydraulics, Delft, The Netherlands.

Skafel, M.G. and Krishnappan, B.G., 1984, Suspended Sediment Distribution in Wave Field, Journal of Waterway, Port, Coastal and Ocean Engineering, Vol. 110, No. 2.

Staub, C., Jonsson, I.G. and Svendsen, I.A., 1984, Variation of Sediment Suspension in Oscillatory Flow, Coastal Engineering, Houston, USA.

Swart, H., 1976, Predictive Equations Regarding Coastal Transports, Coastal Eng. Conference, Honolulu, Hawaii.

Swart, H., 1976, Computation of Longshore Transport, Delft Hydraulics, Report R968-I, Delft, The Netherlands.

Van der Velden, E., 1986, Sediment Suspension in an Oscillating Flow near the Bed, Delft Univ. of Technology, Coastal Egn. Dep., Delft, The Netherlands.

Van Rijn, L.C., 1984, Sediment Transport, Part II: Suspended Load Transport, Journal of Hydraulic Engineering, ASCE, No. HY11.

Van Rijn, L.C., 1987, Data Base Sand Concentration Profiles for Currents and/or Waves, Report M1695-04-1, Delft Hydraulics, Delft, The Netherlands.

Van Rijn, L.C., 1989, Handbook of Sediment Transport by Currents and Waves, Delft Hydraulics, Delft, The Netherlands.

Van Rijn, L.C., 1990, Principles of Fluid Flow and Surface Waves in Rivers, Estuaries, Seas and Oceans, Aqua Publications, P.O. Box 9896, Amsterdam, The Netherlands.